

# The immunophenotypic and immunogenotypic B-cell differentiation arrest in bone marrow of RAG-deficient SCID patients corresponds to residual recombination activities of mutated RAG proteins

Jeroen G. Noordzij, Sandra de Bruin-Versteeg, Nicole S. Verkaik, Jaak M. J. J. Vossen, Ronald de Groot, Ewa Bernatowska, Anton W. Langerak, Dik C. van Gent, and Jacques J. M. van Dongen

The protein products of the recombination activating genes (*RAG1* and *RAG2*) initiate the formation of immunoglobulin (Ig) and T-cell receptors, which are essential for B- and T-cell development, respectively. Mutations in the *RAG* genes result in severe combined immunodeficiency disease (SCID), generally characterized by the absence of mature B and T lymphocytes, but presence of natural killer (NK) cells. Biochemically, mutations in the *RAG* genes result either in nonfunctional proteins or in proteins with partial recombination activity. The mutated *RAG* genes of 9 patients from 7 families were analyzed for

their recombination activity using extra-chromosomal recombination substrates, rearrangement of endogenous Ig loci in *RAG* gene-transfected nonlymphoid cells, or the presence of Ig gene rearrangements in bone marrow (BM). Recombination activity was virtually absent in all 6 patients with mutations in the *RAG* core domains, but partial activity was present in the other 3 *RAG*-deficient patients, 2 of them having Omenn syndrome with oligoclonal T lymphocytes. Using 4-color flow cytometry, we could define the exact stage at which B-cell differentiation was arrested in the BM of 5 *RAG*-deficient SCID

patients. In 4 of 5 patients, the absence of recombination activity was associated with a complete B-cell differentiation arrest at the transition from cytoplasmic (Cy)  $Ig\mu^-$  pre-B-I cells to  $CyIg\mu^+$  pre-B-II cells. However, the fifth patient showed low frequencies of precursor B cells with  $CyIg\mu$  and surface membrane IgM, in line with the partial recombination activity of the patient's mutated *RAG* gene and the detection of in-frame Ig gene rearrangements in BM. (*Blood*. 2002;100:2145-2152)

© 2002 by The American Society of Hematology

## Introduction

Human severe combined immunodeficiency disease (SCID) refers to a group of disorders, which can be classified based on the pattern of inheritance and the immunologic phenotype.<sup>1</sup> One type of SCID is characterized by autosomal recessive inheritance, absence of T and B lymphocytes in peripheral blood (PB), but presence of natural killer (NK) cells (non-T non-B SCID). A number of patients suffering from non-T non-B SCID carry mutations in the recombination activating genes (*RAG*) 1 or 2.<sup>2</sup> The 2 human *RAG* genes are located in a tail-to-tail orientation on chromosome 11p13 and are expressed during T- and B-cell development in the thymus and bone marrow (BM), respectively.<sup>3-7</sup> The *RAG* proteins are essential to initiate recombination of immunoglobulin (Ig) and T-cell receptor (TCR) loci.<sup>8-10</sup> They introduce double-strand breaks at the recombination signal sequences (RSSs) flanking the variable (V), diversity (D), and joining (J) gene segments, which are then joined to form a V(D)J exon encoding the antigen-binding part of Ig and TCR molecules.<sup>11,12</sup>

The *RAG1* and *RAG2* proteins both contain a core domain, which is essential for recombination activity.<sup>13-16</sup> Although the N-terminus of *RAG1* and the C-terminus of *RAG2* seem to be dispensable for recombination activity, it has been shown that they

might be specifically required for Ig gene recombination.<sup>17-21</sup> Most mutations in the *RAG* genes causing non-T non-B SCID affect the core domain and encode nonfunctional proteins ("null" alleles).<sup>2</sup> On the other hand, some *RAG* mutations in the core domain are associated with partial VDJ recombination activity, causing a variant of non-T non-B SCID, called Omenn syndrome (OS).<sup>22</sup> OS is characterized by oligoclonal, autoreactive T cells with a T-helper 2 phenotype, absence of B lymphocytes, but high serum IgE levels. The clinical phenotype of OS resembles the clinical phenotype resulting from maternal-fetal T-cell engraftment (MFT) in a newborn with non-T non-B SCID.

The absence of T or B lymphocytes (or both) in the PB of patients suffering from *RAG*-deficient SCID results from a differentiation arrest during T- and B-cell development in the thymus and BM, respectively. The localization of this differentiation arrest has been defined in murine thymus and BM.<sup>23,24</sup> However, no such data are available in humans. From a theoretical viewpoint, one would expect that *RAG*-deficient SCID patients have a complete B-cell differentiation arrest at the transition from cytoplasmic (Cy)  $Ig\mu^-$  to  $CyIg\mu^+$  precursor B cells, but this has not been shown yet.<sup>25</sup> Here we present data on 9 *RAG*-deficient SCID patients from

From the Department of Immunology, Erasmus MC, University Medical Center Rotterdam, Rotterdam, The Netherlands; Department of Pediatrics, Division of Immunology and Infectious Diseases, Erasmus MC, University Medical Center Rotterdam, Rotterdam, The Netherlands; Department of Cell Biology and Genetics, Erasmus MC, University Medical Center Rotterdam, Rotterdam, The Netherlands; Department of Pediatrics, Leiden University Medical Center, Leiden, The Netherlands; and Department of Immunology, The Children's Memorial Health Institute, Warsaw, Poland.

Supported by Revolving Fund project of the University Hospital Rotterdam, The Netherlands.

**Reprints:** Jacques J. M. van Dongen, Department of Immunology, Erasmus MC, University Medical Center Rotterdam, dr. Molewaterplein 50, 3015 GE Rotterdam, The Netherlands; e-mail: vandongen@immu.fgg.eur.nl.

The publication costs of this article were defrayed in part by page charge payment. Therefore, and solely to indicate this fact, this article is hereby marked "advertisement" in accordance with 18 U.S.C. section 1734.

© 2002 by The American Society of Hematology

Submitted August 16, 2001; accepted May 3, 2002.

7 families. The recombination activity of the mutated *RAG* genes was analyzed using extrachromosomal recombination substrates, rearrangement of endogenous Ig loci in (mutated) *RAG* gene-transfected human nonlymphoid cells, or the occurrence of Ig gene rearrangements (immunogenotype) in BM of the SCID patients. In addition, from 5 *RAG*-deficient SCID patients, the composition of the precursor B-cell compartment in BM could be analyzed with 4-color flow cytometric immunophenotyping.

## Materials and methods

### Cell samples

Over the last 15 years, we received BM samples from 7 B cell-negative SCID patients, and Epstein-Barr virus (EBV)-transformed B-cell lines derived from BM precursor B cells of 2 siblings with B cell-negative SCID.<sup>26</sup>

The BM samples from the 7 SCID patients were subjected to Ficoll-Paque (density: 1.077 g/mL; Pharmacia, Uppsala, Sweden) density centrifugation. The recovered mononuclear cells (MCs) were frozen and stored in liquid nitrogen and thawed later for flow cytometric immunophenotyping studies. Granulocytes were used for DNA extraction.<sup>27</sup>

We have previously reported on an extensive study concerning the composition of the precursor B-cell compartment in the BM of 18 healthy children using triple labelings.<sup>28</sup> We repeated our flow cytometric analyses using quadruple labelings in thawed BM samples from 6 of these healthy children (age range, 1 year 7 months to 5 years 11 months; mean age, 3 years 10 months; 4 boys, 2 girls), who were BM donors for their siblings.

All cell samples were obtained according to the informed consent guidelines of the Medical Ethics Committees of the Leiden University Medical Center and the University Hospital Rotterdam.

### DNA extraction, PCR amplification, and analysis of Ig gene rearrangements

DNA was extracted from BMMCs and transfected  $\phi$ NX-WTA cells (a human epithelial kidney cell line) with the QIAamp Blood kit (Qiagen, Chatsworth, CA).<sup>29</sup> Polymerase chain reaction (PCR) was performed as described previously.<sup>30</sup> In each 100- $\mu$ L PCR 0.1 to 1  $\mu$ g DNA, 10 to 12.5 pmol 5' and 3' oligonucleotides, and 1 U AmpliTaq Gold polymerase (Applied Biosystems, Foster City, CA) were used. Most oligonucleotides for amplification of the *IGH*, *IGK*, and *IGL* genes were published before.<sup>31-33</sup> PCR conditions were 7 minutes at 95°C, followed by 45 seconds at 94°C, 90 seconds at 57 to 65°C, 2 minutes at 72°C for 40 cycles, followed by a final extension step (7 minutes at 72°C). DNA from BMMCs was analyzed for D<sub>H</sub>-J<sub>H</sub> and V<sub>H</sub>-J<sub>H</sub> rearrangements.<sup>32</sup> The PCR products were cloned in the pGEM-T easy vector and subsequently sequenced. When *IGH* rearrangements were identified, DNA from BMMCs was also analyzed for V<sub>K</sub>-J<sub>K</sub> and V <sub>$\lambda$</sub> -J <sub>$\lambda$</sub>  rearrangements.<sup>34</sup> Involved Ig gene segments were identified using IMGT, the international ImMunoGeneTics database <http://imgt.cnusc.fr:8104> (Initiator and coordinator: Marie-Paule Lefranc, Montpellier, France, [lefranc@ligm.igh.cnrs.fr](mailto:lefranc@ligm.igh.cnrs.fr)).<sup>35</sup>

### LR-PCR for amplification of *RAG* genes

The entire *RAG1* or *RAG2* gene was amplified in a single long-range (LR)-PCR reaction (100  $\mu$ L), using 4 U r*Tth* DNA polymerase XL (Applied Biosystems) for subsequent sequencing analysis of the LR-PCR product or 5 U *Pfu* enzyme mix (Stratagene, La Jolla, CA) for cloning the LR-PCR product; we used 30 or 14 pmol oligonucleotides, respectively. The sequences of the oligonucleotides used for the LR-PCR were TGAG-GCTAATACAATGTGGAA (*RAG1* forward), ACAACCTTGGCTTT-GATTTAC (*RAG1* reverse), TTCGGCTAGTCTTTATTAC (*RAG2* forward), and CTTTGGCACATCATTCA (*RAG2* reverse), respectively. Restriction-sites for *Bam*HI and *Not*I were incorporated into the 5' and 3' oligonucleotides used for cloning, respectively. LR-PCR conditions were 2 minutes, 94°C, followed by 15 seconds, 94°C, 30 seconds, 57°C, and 4

minutes, 68°C for 40 cycles using 10-second autoextension from cycle 21 onward. In case of cloning, the LR-PCR conditions were 45 seconds, 94°C, followed by 45 seconds, 94°C, 45 seconds, 62°C, and 3.5 to 6.5 minutes, 72°C for 30 to 35 cycles using 10-sec autoextension from cycle 21 onward. After the last cycle final extension was performed for 10 minutes at 72°C.

### Fluorescent sequencing reaction and analysis

The LR-PCR products of *RAG1* and *RAG2* were purified using QIAquick PCR purification kit (Qiagen). Five to 9  $\mu$ L purified PCR product was sequenced with 5  $\mu$ L dRhodamine dye terminator mix (Applied Biosystems), using 3.3 pmol internal sequencing primers. All sequencing was performed as described before,<sup>32</sup> using an ABI Prism 377 fluorescent sequencer (Applied Biosystems).

### Cloning of mutated and wild-type *RAG* genes

The LR-PCR products containing the entire *RAG1* or *RAG2* open reading frame were isolated after digestion with *Bam*HI and *Not*I and cloned into the *Bam*HI-*Not*I cut vector pEBB under control of the EF-1 promoter.<sup>18</sup> The cloned wild-type and mutated *RAG* genes were sequenced to exclude the presence of PCR-induced mutations.

### V(D)J recombination assay using an extrachromosomal recombination substrate

Two micrograms pEBB-*RAG1* (mutated or wild type) together with 2  $\mu$ g pEBB-*RAG2* (mutated or wild type) and 1  $\mu$ g of the extrachromosomal recombination substrate (pDVG93) were transfected into Chinese hamster ovary (CHO9) cells using SuperFect Transfection Reagent (Qiagen). Transfected cells were cultured for 2 days before harvesting. Plasmid pDVG93 contains 2 RSS elements with the same orientation. On V(D)J recombination, the sequence in between the 2 RSS elements is inverted, which can be detected by PCR.<sup>20</sup> Nontransfected pDVG93 plasmids can be discriminated from transfected plasmids based on digestion of *Dpn*I restriction sites, which become resistant on demethylation after transfection.

A real-time quantitative (RQ)-PCR assay was developed to quantify the recombination activity. For this purpose, we designed primers DG89 and DG147 and TaqMan probe FM23 for quantitative detection of inversional rearrangements as well as a set of control primers and TaqMan probe for quantitative detection of all transfected pDVG93 plasmids with multiple *Dpn*I restriction sites between the primers.<sup>20</sup> DNA recovered from the transfection experiments was *Dpn*I digested to remove nontransfected plasmids, added to the TaqMan universal PCR master mix (Applied Biosystems), and equally divided over 4 tubes, 2 tubes for specific amplification and 2 for control amplification. RQ-PCR was performed as described before using an ABI Prism 7700 (Applied Biosystems).<sup>36</sup> The PCR cycle at which a fluorescent signal became detectable (threshold cycle or C<sub>T</sub>) was comparable in the duplicate tubes ( $\Delta$ C<sub>T</sub> < 1.0). The level of recombination activity of the mutated *RAG* genes was compared to that of wild-type *RAG* genes. All RQ-PCR experiments were performed multiple times, showing virtually identical results.

Transfection of wild-type *RAG* genes was used as a positive control for recombination activity. Using these RQ-PCR results, standard curves for the specific and the control amplification were generated. All standard curves met the following requirements: slopes between -3.3 and -3.7 to ensure optimal amplification, correlation coefficient close to 1.0, and a fluorescent signal intensity ( $\Delta$ Rn) greater than 1.0. Using the relative standard curve method with separate tubes (Applied Biosystems, user bulletin no. 2, relative quantitation of gene expression), the relative recombination activity of the wild-type *RAG* genes was arbitrarily set to 100%. The relative recombination activity of mutated *RAG* genes was calculated from the specific standard curve and corrected using the control standard curve.

### Analysis of V(D)J recombination of endogenous Ig loci following transfection of cloned *RAG* genes in combination with E47 in $\phi$ NX-WTA cells

Transfection was performed as described before.<sup>37</sup> In short, 6  $\mu$ g pEBB-*RAG1* (mutated or wild type) together with 6  $\mu$ g pEBB-*RAG2* (mutated or

wild type) and 6  $\mu\text{g}$   $\beta\text{HAP-E47}$  (under control of the human  $\beta$ -actin promoter) were transfected into confluent  $\phi\text{NX-WTA}$  human kidney epithelial cells using the calcium-phosphate method.<sup>37</sup> Transfected cells were cultured for 3 days before harvesting. DNA was isolated and analyzed for rearrangement of endogenous loci, such as  $\text{D}_{\text{H}4\text{-J}_{\text{H}}}$ ,  $\text{V}_{\text{K}1\text{-J}_{\text{K}}}$ , and  $\text{V}_{\lambda 3\text{-J}_{\lambda 1/2/3}}$ . These rearrangements were earlier shown to be specifically induced on transfection of E47 and RAG1 and RAG2.<sup>37</sup>

### Flow cytometric analysis of BM samples from healthy children and SCID patients

Fifty-microliter aliquots of thawed BMSCs ( $10 \times 10^6$  cells/mL) were incubated for 10 minutes at room temperature with combinations of optimally titrated monoclonal antibody (mAb): 50  $\mu\text{L}$  fluorescein isothiocyanate (FITC)-conjugated mAb, 50  $\mu\text{L}$  phycoerythrin (PE)-conjugated mAb, 50  $\mu\text{L}$  peridinin chlorophyll protein-cyanin 5.5 (PerCP-Cy5.5)-conjugated mAb, and 50  $\mu\text{L}$  allophycocyanin (APC)-conjugated mAb were used to detect membrane-bound antigens. After incubation, the cells were washed and further processed depending on the type of quadruple labeling. The 14 applied quadruple labelings are summarized on a Web page (<http://www.eur.nl/fgg/immu/tables/Table1.htm>).

Quadruple labelings for membrane-bound antigens (labelings 1-7) were directly analyzed by flow cytometry using FACSCalibur (Becton Dickinson, San Jose, CA). For quadruple labelings involving intracellular staining of Cy CD79a, CyIg $\mu$ , and CyVpreB,<sup>38</sup> and intranuclear staining of terminal deoxynucleotidyl transferase (TdT) (labelings 8-14), we first performed the membrane labelings, followed by permeabilization of the BM cells using IntraPrep Permeabilization Reagent (Immunotech, Marseille, France), and subsequent intracellular staining.<sup>39,40</sup>

## Results

### Patient characteristics and mutations in the RAG genes

Based on clinical characteristics and immunophenotyping results of PB, 9 patients from 7 families were diagnosed as having B cell-negative SCID (Table 1). SCID-1 was studied extensively and published before.<sup>20</sup> MFT in patients diagnosed with OS (SCID-1 and SCID-5) was excluded by HLA typing and by detection of a homozygous RAG gene mutation in PBMC DNA.

We detected mutations in the RAG1 or RAG2 genes in all 9 B cell-negative SCID patients (Table 1). The RAG1 genes contained 4 different mutations, including one novel. Two of the 4 mutations (Arg249His and Lys820Arg) represented polymorphisms. The Arg249His mutation has been shown to be a functionally intact polymorphism by recombination activity studies,<sup>2</sup> whereas the Lys820Arg mutation was interpreted as a polymorphism based on its allelic frequency.<sup>41</sup> In this study, we show that the Lys820Arg mutation indeed retained intact recombination activity (see below).

The other 2 RAG1 mutations (codon 199 stop in SCID-1 and Arg404Gln in SCID-7), were shown by recombination activity studies (see below) to have a disease-causing effect.

We detected 4 different mutations in the RAG2 genes, including 3 novel mutations (Table 1). The disease-causing effect of the 3 novel mutations (codon 247 stop in SCID-2 and SCID-4, His481Pro in SCID-3, and Gln16 stop in SCID-6) was shown by recombination activity studies (see below). It has been shown before that the Trp453Arg mutation in SCID-5 retained partial RSS nicking and hairpin formation function, as well as a reduced capacity to form signal and coding joints, compatible with the clinical diagnosis of OS in SCID-5 (Table 1).<sup>42</sup> For this reason, we did not clone the Trp453Arg mutation for recombination studies.

According to the information obtained by the clinicians, families SCID-2 and SCID-4 were unrelated. Nevertheless, we identified the same disease-causing mutation in RAG2 (codon 247 stop) and the same polymorphism in RAG1 (Lys820Arg) in both families.

### V(D)J recombination activity

After transfection, plasmid pDVG93 was used as template for PCR and subsequent hybridization with a radioactive probe (results not shown), as well as for RQ-PCR reaction after digestion with the restriction enzyme *DpnI*. The results of the RQ-PCR reaction are shown in Table 2. Transfection of the wild-type RAG1 gene or the Lys820Arg mutation resulted in identical amplification curves. After correction for transfection efficiency and the amount of pDVG93 added to the RQ-PCR reaction, the relative recombination activities were comparable, indicating that the Lys820Arg mutation represents a functional polymorphism.

After correction for transfection efficiency and the amount of pDVG93 added to the RQ-PCR reaction, the mutated RAG genes of SCID-1 and SCID-3 showed the highest residual recombination activities (Table 2). SCID-1 suffered from an OS-like T<sup>+</sup>/B<sup>-</sup> SCID.<sup>20</sup> The RAG1 631delT mutation in this patient was shown to result in an N-terminal truncation of RAG1, leaving the core domain unaffected.<sup>20</sup> SCID-3 suffered from a genuine non-T, non-B SCID. The amino acid substitution (His481Pro) in this patient was located outside the core domain in the C-terminus of RAG2. The RAG core domain mutations in SCID-2, SCID-4, SCID-6, and SCID-7 resulted in very low relative recombination activities (Table 2). It has been published recently that a RAG1 Arg404Trp mutation (comparable to the Arg404Gln mutation in SCID-7) resulted in complete absence of recombination activity as well.<sup>43</sup>

**Table 1. Mutation analysis in patients presenting with B cell-negative SCID**

Family	Diagnosis*	Mutation		Polymorphism		Consanguinity of parents
		DNA level†	Protein level	DNA level†	Protein level	
RAG-SCID 1	OS	RAG1 631delT§	Codon 199 stop	RAG1 G858A§	Arg249His	Yes
RAG-SCID 2‡	T <sup>-</sup> B <sup>-</sup> SCID	RAG2 1913delG§	Codon 247 stop	RAG1 A2571G§	Lys820Arg	Yes
RAG-SCID 3	T <sup>-</sup> B <sup>-</sup> SCID	RAG2 A2643C	His481Pro			Yes
RAG-SCID 4‡	T <sup>-</sup> B <sup>-</sup> SCID	RAG2 1913delG	Codon 247 stop	RAG1 A2571G	Lys820Arg	Unknown
RAG-SCID 5	OS	RAG2 T2558A§	Trp453Arg	RAG1 G858A§	Arg249His	No
RAG-SCID 6	T <sup>-</sup> B <sup>-</sup> SCID	RAG2 C1247T	Gln16 stop			No
RAG-SCID 7	T <sup>-</sup> B <sup>-</sup> SCID	RAG1 G1323A	Arg404Gln	RAG1 G858A	Arg249His	No

\*Diagnoses were obtained in PB.

†Numbering of RAG1 gene according to Schatz et al,<sup>3</sup> RAG2 gene according to Ichihara et al.<sup>5</sup>

‡Patients from different families with identical mutations.

§Homozygous mutation, both parents were carrier.

||Seemingly homozygous mutation, but deletion of the other allele was not ruled out.

**Table 2. Relative recombination activity of mutated RAG genes**

Patient	RAG1 protein	RAG2 protein	Relative recombination activity using pDVG93 (%)*	E47 induced rearrangements of endogenous loci in $\phi$ NX-WTA cells		
				V <sub>K</sub> 1-J <sub>K</sub>	D <sub>H</sub> 4-J <sub>H</sub>	V <sub>λ</sub> 3-J <sub>λ</sub>
Healthy control	Wild type	Wild type	100	+	+	+
RAG-SCID 1	N-terminal truncation	Wild type	9.3 ± 2.9	+	-	+
RAG-SCID 2 and 4	Lys820Arg	Codon 247 stop	1.4 ± 1.6	-	-	-
	Lys820Arg	Wild type	115.1 ± 54.4	+	+	+
	Wild type	Codon 247 stop	1.6 ± 2.4	-	-	-
RAG-SCID 3	Wild type	His481Pro	3.2 ± 2.0	+	-	+
RAG-SCID 6	Wild type	Gln16 stop	0	-	-	-
RAG-SCID 7	Arg404Gln	Wild type	1.3 ± 1.5	-	-	-
Mock transfection†	—	—	0	-	-	-

\*Mean of 4 RQ-PCR reactions using plasmids from 4 different transfections.

†Mock transfection consisted of H<sub>2</sub>O in case of transfection of CHO9 cells and of E47 without wt RAG genes in case of transfection of  $\phi$ NX-WTA cells.

### Rearrangement of endogenous Ig loci after transfection of $\phi$ NX-WTA human kidney epithelial cells

To study the ability of mutated RAG genes to rearrange endogenous Ig loci, we transfected wild-type or mutated RAG genes together with transcription factor E47 in  $\phi$ NX-WTA cells.  $\phi$ NX-WTA cells are human kidney epithelial cells that do not express RAG proteins and for this reason provide a good model system to study the effect of cloned RAG mutations. Transfection of E47 together with wild-type RAG genes was shown to specifically induce D<sub>H</sub>4-J<sub>H</sub>, V<sub>K</sub>1-J<sub>K</sub>, and V<sub>λ</sub>3-J<sub>λ</sub> rearrangements.<sup>37</sup> Therefore, we analyzed the occurrence of these rearrangements in our transfection assay (Table 2). Transfection of E47 without wt RAG genes did not result in rearrangements.

The mutated RAG genes of SCID-1 and SCID-3 with the highest relative recombination activity in the extrachromosomal recombination assay were also able to perform V<sub>K</sub>1-J<sub>K</sub> and V<sub>λ</sub>3-J<sub>λ</sub> rearrangements when cotransfected with E47 (Table 2). Except for the Lys820Arg polymorphism in RAG1, we could not detect D<sub>H</sub>4-J<sub>H</sub> rearrangements after transfection of mutated RAG genes.

### Ig gene rearrangements in BMMCs

To study the in vivo capacity of mutated RAG genes to rearrange Ig loci during human B-cell differentiation, DNA was isolated from BMMCs of several RAG-deficient SCID patients and investigated for the occurrence of incomplete D<sub>H</sub>-J<sub>H</sub> and complete V<sub>H</sub>-J<sub>H</sub>

rearrangements. IGH rearrangements were detected in only 2 of 7 RAG-deficient SCID patients studied (Table 3), the same patients (SCID-1 and SCID-3) who were shown to harbor partial recombination activity (Table 2). The 2 patients with IGH rearrangements were also analyzed for the presence of IGK and IGL rearrangements. As expected in patients suffering from RAG-deficient SCID, no somatic mutations could be detected (Table 3).

Patients SCID-7.1 and 7.2 were 2 sisters suffering from the same RAG1 mutation. This Arg404Gln mutation was shown to cause a complete loss of function (Table 2). The EBV-transformed B-cell lines of both patients were reported to have germline IGH, IGK, and IGL genes, as assessed by Southern blotting.<sup>26</sup>

### Composition of the BM lymphocyte gate and design of an optimal B-cell gate

As shown previously, the composition of the BM lymphocyte gate in healthy children is highly variable, because of "contamination" with T lymphocytes, NK cells, myeloid precursors, and normoblasts.<sup>28</sup> Therefore, reliable comparison of B-cell subpopulations in BM samples from healthy children and RAG-deficient SCID patients requires analysis within a well-defined and "purified" B-cell gate (Figures 1 and 2).

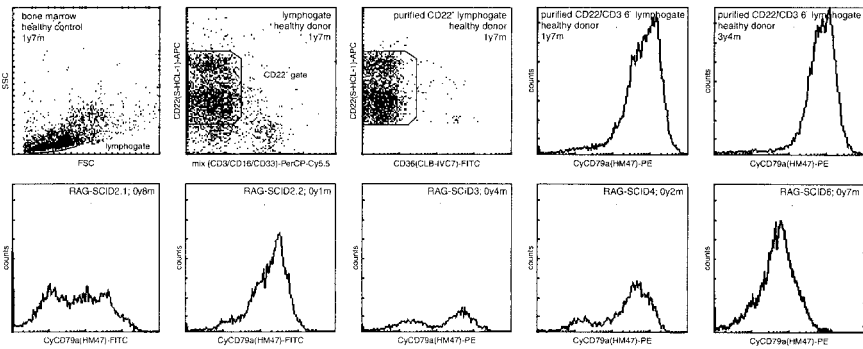
During our initial flow cytometric analyses of SCID BM samples, we detected coexpression of CD36 and the pan B-cell markers CD22, CyCD79a, and CD19 in SCID patients and

**Table 3. Analysis of IGH, IGK, and IGL gene rearrangements in BMMCs of RAG-deficient SCID patients**

Patient	Origin of DNA	Analyzed gene	PCR products	V gene segment	Junctional region		D gene segment	J gene segment	Junctional region	J gene segment	Frame	Somatic mutations	No. of identical clones		
					Del	Del								Del	Del
RAG-SCID 1	BMMC	IGH	Identified				D <sub>H</sub> 2-15	- 5	T	- 2	J <sub>H</sub> 4	NA	NA	1	
		IGK	Not identified												
RAG-SCID 3	BMMC	IGL	Identified	V <sub>λ</sub> 2	- 4	CCT	-	-	-	0	J <sub>λ</sub> 3	+	Absent	1	
		IGH	Identified	V <sub>H</sub> 3-7	0	TTGTA	- 2	D <sub>H</sub> 3-22	0	-	- 1	J <sub>H</sub> 3b	+	Absent	4
				V <sub>H</sub> 5-51	- 1	GC	- 1	D <sub>H</sub> 2-15/INV	- 15	GGGCTACGGGG	- 6	J <sub>H</sub> 4b	+	Absent	6
								D <sub>H</sub> 3-10	- 7	G	- 11	J <sub>H</sub> 2	NA	NA	4
								D <sub>H</sub> 2-21	- 7	AAGAC	- 4	J <sub>H</sub> 3b	NA	NA	1
								D <sub>H</sub> 4-23	- 3	GACTGCGA	- 11	J <sub>H</sub> 4	NA	NA	1
								D <sub>H</sub> 4-17	- 1	ACTAG	- 4	J <sub>H</sub> 5	NA	NA	3
		IGK	Not identified												
		IGL	Identified	V <sub>λ</sub> 3-10*01	0	-	-	-	-	0	J <sub>λ</sub> 3*01	+	Absent	3	

PCR products of the IGH gene could not be identified using DNA from BMMCs in patients RAG-SCID 2.1, 2.2, 4, 5, and 6. Del indicates deletion of germline gene segment nucleotides; NA, not applicable; INV, inverted.

**Figure 1. BM samples of RAG-deficient SCID patients contained increased numbers of the most immature CD22<sup>+</sup>/CyCD79a<sup>-</sup> pro-B cells.** CyCD79a expression of the precursor B-cell compartment was analyzed within a lymphocyte gate and a CD22<sup>+</sup> gate, which was "purified" by exclusion of cells with expression of CD3, CD16, or CD33. In healthy children the CD22<sup>+</sup>/CyCD79a<sup>-</sup> pro-B-cell subset represented a minor fraction of the total precursor B-cell compartment. In most RAG-deficient SCID patients this CyCD79a<sup>-</sup> subset was relatively large but variable in size. Furthermore, the level of CyCD79a expression in the SCID patients (mainly pre-B-I cells) was lower than in the healthy controls (mainly pre-B-II cells and immature B cells). The age at BM sampling is indicated.



virtually not in healthy controls. CD36 is expressed on platelets, mature monocytes, and macrophages, during stages of erythroid cell development and on some macrophage-derived dendritic cells. Therefore, we added CD36 as exclusion marker to some essential labelings (labelings 5, 10, and 14; see <http://www.eur.nl/fgg/immu/tables/Table1.htm>), resulting in increased purity of the B-cell gates. We have shown previously that CD22 is a reliable pan B-cell marker, which is rarely expressed on CD3<sup>+</sup> T cells, CD33<sup>+</sup> myeloid cells, or CD16<sup>+</sup> NK cells.<sup>28</sup> We identified the entire B-cell compartment as being CD22<sup>+</sup>. In healthy children the CyCD79a<sup>+</sup> and the CD19<sup>+</sup> fractions within the CD22<sup>+</sup> B-cell compartment were very large (labelings 5 and 14; see Web page), that is, 98.7%

and 97.6%, respectively. The percentages of the different subpopulations within the CyCD79a<sup>+</sup> or CD19<sup>+</sup> gates were recalculated into percentages of the CD22<sup>+</sup> population, by multiplying with 0.987 and 0.976, respectively. The same approach was followed for SCID patients, who contained a substantially larger fraction of CD22<sup>+</sup>/CyCD79<sup>-</sup> pro-B cells (Figure 1).

**B-cell subsets in BM from healthy donors**

Based on detailed triple flow cytometric labelings, we previously presented the composition of the precursor B-cell compartment in healthy children and found that its composition is stable during

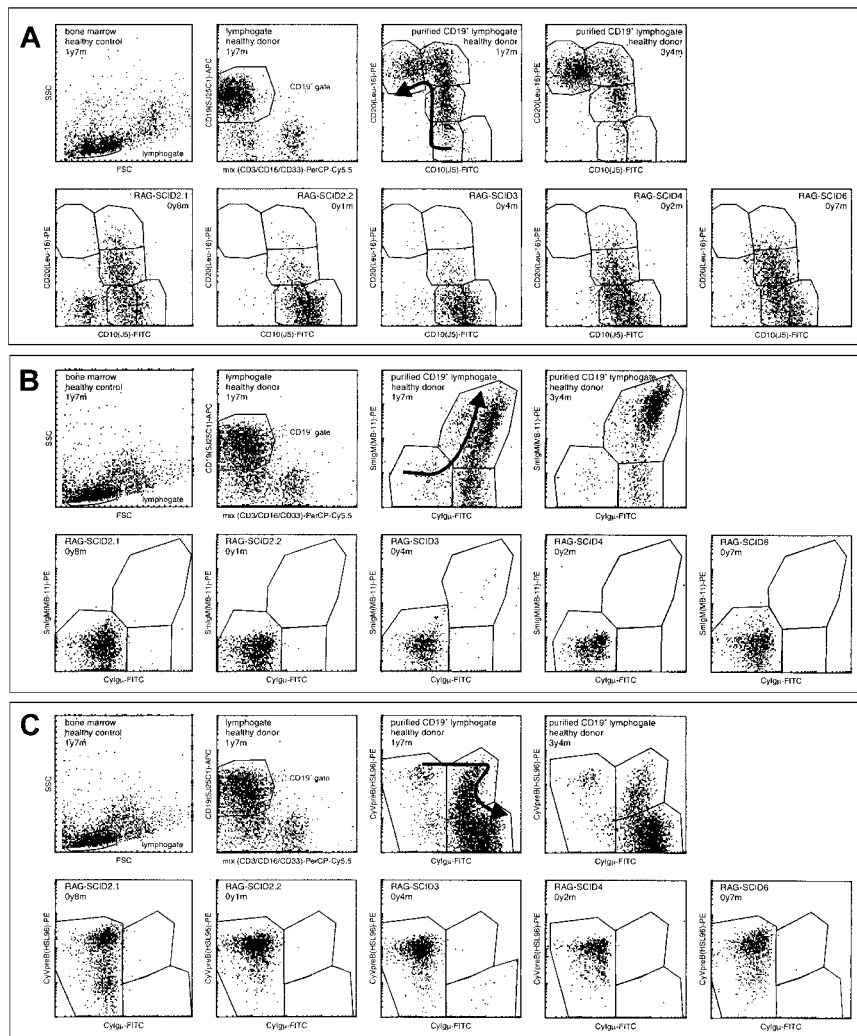


**Figure 2. Flow cytometric analysis of thawed BM samples from 5 RAG-deficient SCID patients compared to 2 healthy children.** The precursor B-cell compartment was analyzed within a lymphocyte gate and a CD19<sup>+</sup> gate, which was purified by exclusion of cells expressing CD3, CD16, or CD33. (A) Analysis of CD10 and CD20 expression within the purified CD19<sup>+</sup> lymphocyte gate. (B) Analysis of CyIgμ and SmlgM expression within the purified CD19<sup>+</sup> lymphocyte gate. (C) Analysis of CyIgμ and CyVpreB expression within the purified lymphocyte gate. The sequential order of the B-cell differentiation stages is indicated with arrows in the youngest healthy child. The composition of the precursor B-cell compartment in the 2 healthy children was representative of that in other healthy children (n = 6). In general, RAG-deficient SCID patients lacked the more mature B-cell differentiation stages with a strong relative increase in the immature B-cell differentiation stages. According to Nomura et al, expression of CyVpreB precedes expression of CD19.<sup>45</sup> Within a CD19<sup>+</sup> lymphocyte gate, all cells should thus be CyVpreB<sup>+</sup> or CyIgμ<sup>+</sup> (C). Therefore, we suggest that the double-negative events represent apoptotic cells. The age at BM sampling is indicated.

childhood.<sup>28,44</sup> Because we now extended our flow cytometric protocol to 14 quadruple labelings, we have repeated our flow cytometric analyses on thawed BM samples from 6 of the previously studied healthy children, resulting in the recognition of 9 consecutive stages. We have previously compared the composition of the precursor B-cell compartment in fresh BM and thawed BM samples from healthy children and we could not detect major selective loss of particular precursor B-cell subsets.<sup>28</sup>

The mature B-cell population in BM varied between healthy children mainly because of blood contamination with CD10<sup>-</sup>/SmIgM<sup>+</sup>/SmIgD<sup>+</sup> B lymphocytes.<sup>28</sup> To correct for this variance in our comparative studies between precursor B cells in normal BM and in BM from SCID patients, we excluded the mature CD10<sup>-</sup>/SmIgM<sup>+</sup>/SmIgD<sup>+</sup> B-cell population (stage 9) from our calculations. Consequently, the percentages of stages 1 to 8 were recalculated and set at 100% (Figure 3).

### Flow cytometric analysis of precursor B cells in BM of SCID patients

The BM samples from 7 RAG-deficient SCID patients were available, but BM samples from OS patients SCID-1 and SCID-5 could not be analyzed using flow cytometry due to the very low percentage of precursor B cells (< 2% CD22<sup>+</sup>/CD36<sup>-</sup> precursor B cells within the lymphocyte gate).

In BM from healthy children, approximately 15% of the precursor B-cell compartment consisted of CyIgμ<sup>-</sup> precursor B cells, whereas in BM from all 5 analyzed RAG-deficient SCID patients approximately 99% (97%-100%) of the precursor B-cell compartment was located in these stages (Figure 3). Although this differentiation arrest was virtually identical in the 5 evaluated SCID patients, some CyIgμ<sup>+</sup> pre-B-II cells and SmIgM<sup>+</sup> immature B cells could be detected in SCID-3 (Figures 2 and 3). Furthermore, the composition of the remaining precursor B-cell compartment (pro-B cell and pre-B-I cell subsets) in the 5 SCID patients was highly variable, even in the 3 patients with the same homozygous RAG2 mutation (SCID-2.1, 2.2, and 4).

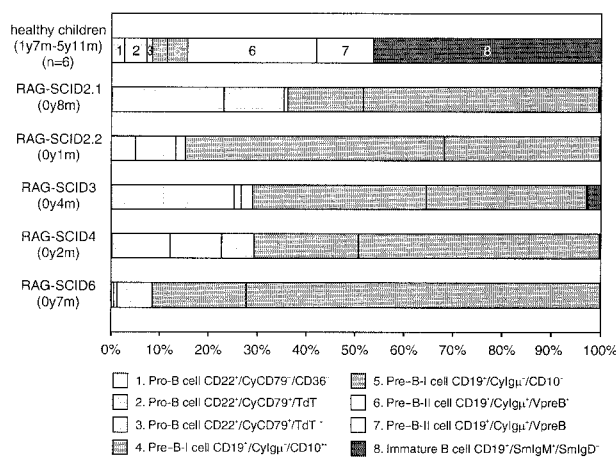


**Figure 3. Composition of the precursor B-cell compartment in RAG-deficient SCID patients compared with healthy children.** The precursor B-cell compartment was set at 100% after exclusion of CD10<sup>-</sup>/SmIgM<sup>+</sup>/SmIgD<sup>+</sup> mature B cells.<sup>28</sup> All RAG-deficient SCID patients showed a similar differentiation arrest with approximately 99% of the precursor B cells in the pro-B and pre-B-I stages (stages 1-5), thereby revealing an arrest at the transition from CyIgμ<sup>-</sup> pre-B-I (stages 4 and 5) to CyIgμ<sup>+</sup> pre-B-II-cells (stages 6 and 7, white bars). Only in SCID-3 was some leakiness observed with more than 3% Ig<sup>+</sup> B cells. These Ig<sup>+</sup> B cells were mainly SmIgM<sup>+</sup> immature B cells (stage 8, dark bar), which is also shown in Figure 2B. The age of BM sampling is indicated.

## Discussion

We have identified 9 patients from 7 families with B cell-deficient SCID due to RAG mutations. The mutations in the RAG genes of SCID-2, SCID-4, SCID-6, and SCID-7 affected the core domains of the RAG proteins and were shown to abrogate recombination activity (almost) completely. The other 3 RAG mutations were located outside the core domain (SCID-1, SCID-3, and SCID-5) and were all associated with partial recombination activity (Table 4). The partial recombination activity was reported previously for the Trp453Arg RAG2 mutation of OS patient SCID-5,<sup>42</sup> whereas the mutated RAG genes of SCID-1 and SCID-3 were shown to have partial recombination activity in our extrachromosomal recombination assay. In line with some remaining recombination activity of the C-terminal mutated RAG2 protein in SCID-3, some SmIgM<sup>+</sup> immature B cells were detectable in the BM of this patient (Figures 2 and 3). Consequently, complete and in-frame IGH and IGL rearrangements were detectable in the BM precursor B cells (Table 3). The amino acid substitution in the C-terminus of the RAG2 protein in SCID-3 was located outside the functionally important core domain, but this mutation might result in diminished protein stability, thereby explaining the strongly reduced recombination activity.

We found that approximately 99% (97%-100%) of the precursor B-cell compartment in the SCID patients consisted of CyIgμ<sup>-</sup> precursor B cells (pro-B cells and pre-B-I cells), in contrast to approximately 15% in healthy children. The localization of the virtually complete arrest at the transition between CyIgμ<sup>-</sup> and CyIgμ<sup>+</sup> pre-B cells in all 5 RAG-deficient SCID patients is in line with the essential role of the RAG proteins in initiation of the VDJ recombination process. This contrasts with the leakiness of the B-cell differentiation arrest in patients with X-linked agammaglobulinemia (XLA).<sup>28,45</sup> Only in SCID-3 some minor leakiness was seen (3% Ig<sup>+</sup> B cells and detectable Ig gene rearrangements), which was clearly related to the low levels of recombination activity. These data show that in RAG-deficient SCID patients the immunophenotypic and immunogenotypic B-cell differentiation arrests are closely linked (Table 4).

As was observed earlier, a small subpopulation of CD34<sup>+</sup>/CD20<sup>+</sup> precursor B cells was detectable within the CD19<sup>+</sup> gate in BM from healthy children.<sup>28</sup> However, in BM from most SCID patients a substantial CD34<sup>+</sup>/CD20<sup>+</sup>/CD19<sup>+</sup> population could be identified. We observed that the CD34<sup>+</sup>/CD20<sup>+</sup> population is also relatively large in the precursor B-cell compartment of XLA patients, suggesting that down-regulation of CD34 is normally associated with pre-BCR signaling.<sup>28</sup>

We observed that CD36 coexpressed with the pan B-cell markers CD22, CyCD79a, and CD19 on BM cells in SCID patients, but virtually not in healthy controls. We also detected coexpression of these markers on BM cells of XLA patients. The CD36<sup>+</sup>/CD22<sup>+</sup> cells might represent early myeloid-lymphoid precursor cells, which are detectable in BM of SCID and XLA patients due to the relative increase in early precursor B cells. However, so far we have no explanation for the coexpression of CD36 and the slightly later expressed pan B-cell markers CyCD79a and CD19.

Although it has been shown that OS is caused by mutated RAG genes with partial recombination activity,<sup>22</sup> it is not understood why these patients present with oligoclonal T lymphocytes, in the absence of B lymphocytes. The presence of high serum IgE levels

**Table 4. Summary of RAG gene mutations, their recombination activity, and effects on the in vivo lymphoid compartment**

Gene	Mutation	Recombination activity	Diagnosis*	Lymphoid compartment		
				Precursor B cells in BM		Immunogenotype
				Relative size	Differentiation arrest	
RAG1	N-terminal truncation	Strongly decreased	OS in SCID-1	< 2%	Not evaluable	Oligoclonal T cells
	Arg249His	Normal (polymorphism)				
	Arg404Gln	Absent	T <sup>-</sup> B <sup>-</sup> in SCID-7	No BM available		No Ig rearrangements†
RAG2	Lys820Arg	Normal (polymorphism)				
	Gln16 stop	Absent	T <sup>-</sup> B <sup>-</sup> in SCID-6	57%	Absolute arrest	No Ig rearrangements
	Codon 247 stop	Absent	T <sup>-</sup> B <sup>-</sup> in SCID-2 and -4	5%-57%‡	Absolute arrest	No Ig rearrangements
	Trp435Arg	Strongly decreased§	OS in SCID-5	< 2%	Not evaluable	Oligoclonal T cells
	His481Pro	Strongly decreased	T <sup>-</sup> B <sup>-</sup> in SCID-3	4%	Leakiness	IGH/IGL rearrangements

\*The immunophenotype was obtained from PB.

†The immunogenotype in SCID-7 was detected in EBV-transformed B-cell lines.

‡5% within lymphocyte gate in SCID-2.1, 57% in SCID-2.2, and 47% in SCID-4.

§The recombination activity in SCID-5 was taken from the literature.<sup>42</sup>

suggests that Ig-producing plasma cells might be present in patients with OS. However, in BM samples from 2 patients with OS (SCID-1 and SCID-5), flow cytometric analysis was impossible because the percentage CD22<sup>+</sup>/CD36<sup>-</sup> precursor B cells was less than 2% of lymphocytes, revealing a severe suppression of the B-cell compartment. One would expect OS patients to have the same percentage of precursor B cells as other RAG-deficient SCID patients, but this was not the case in our OS patients. This might at least partly be caused by the relatively high frequency of oligoclonal T cells within the BM lymphocyte gate (73% and 67% in our OS patients).

In conclusion, we observed a complete B-cell differentiation arrest at the pre-BCR checkpoint in the BM of RAG-deficient SCID patients with absence of recombination activity. One patient

(SCID-3) showed some SmIgM<sup>+</sup> immature B cells, which corresponded with partial recombination activity of the mutated RAG2 protein and the presence of in-frame Ig gene rearrangements. The partial recombination activity in 2 other patients was associated with OS and oligoclonal T cells.

## Acknowledgments

The authors thank Dr H. Karasuyama for making available the monoclonal antibody HSL96 directed against the human VpreB protein, and Miss G. van der Linden and Miss K. Wiertz for technical assistance.

## References

- Buckley RH, Schiff RI, Schiff SE, et al. Human severe combined immunodeficiency: genetic, phenotypic, and functional diversity in one hundred eight infants. *J Pediatr*. 1997;130:378-387.
- Schwarz K, Gauss GH, Ludwig L, et al. RAG mutations in human B cell-negative SCID. *Science*. 1996;274:97-99.
- Schatz DG, Oettinger MA, Baltimore D. The V(D)J recombination activating gene, RAG-1. *Cell*. 1989;59:1035-1048.
- Oettinger MA, Stanger B, Schatz DG, et al. The recombination activating genes, RAG 1 and RAG 2, are on chromosome 11p in humans and chromosome 2p in mice. *Immunogenetics*. 1992;35:97-101.
- Ichihara Y, Hirai M, Kurosawa Y. Sequence and chromosome assignment to 11p13-p12 of human RAG genes. *Immunol Lett*. 1992;33:277-284.
- Huppi K, Siwarski D, Shaughnessy J Jr, et al. Genes associated with immunoglobulin V(D)J recombination are linked on mouse chromosome 2 and human chromosome 11. *Immunogenetics*. 1993;37:288-291.
- Schwarz K, Hameister H, Gessler M, Grzeschik KH, Hansen-Hagge TE, Bartram CR. Confirmation of the localization of the human recombination activating gene 1 (RAG1) to chromosome 11p13. *Hum Genet*. 1994;93:215-217.
- Oettinger MA, Schatz DG, Gorka C, Baltimore D. RAG-1 and RAG-2, adjacent genes that synergistically activate V(D)J recombination. *Science*. 1990;248:1517-1523.
- McBlane JF, Van Gent DC, Ramsden DA, et al. Cleavage at a V(D)J recombination signal requires only RAG1 and RAG2 proteins and occurs in two steps. *Cell*. 1995;83:387-395.
- Van Gent DC, McBlane JF, Ramsden DA, Sadofsky MJ, Hesse JE, Gellert M. Initiation of V(D)J recombination in a cell-free system. *Cell*. 1995;81:925-934.
- Van Gent DC, Ramsden DA, Gellert M. The RAG1 and RAG2 proteins establish the 12/23 rule in V(D)J recombination. *Cell*. 1996;85:107-113.
- Eastman QM, Leu TM, Schatz DG. Initiation of V(D)J recombination in vitro obeying the 12/23 rule. *Nature*. 1996;380:85-88.
- Sadofsky MJ, Hesse JE, McBlane JF, Gellert M. Expression and V(D)J recombination activity of mutated RAG-1 proteins. *Nucleic Acids Res*. 1993;21:5644-5650.
- Sadofsky MJ, Hesse JE, Van Gent DC, Gellert M. RAG-1 mutations that affect the target specificity of V(D)J recombination: a possible direct role of RAG-1 in site recognition. *Genes Dev*. 1995;9:2193-2199.
- Kirch SA, Sudarsanam P, Oettinger MA. Regions of RAG1 protein critical for V(D)J recombination. *Eur J Immunol*. 1996;26:886-891.
- Steen SB, Han JO, Mundy C, Oettinger MA, Roth DB. Roles of the "dispensable" portions of RAG-1 and RAG-2 in V(D)J recombination. *Mol Cell Biol*. 1999;19:3010-3017.
- McMahan CJ, Difiilippantonio MJ, Rao N, Spanopoulou E, Schatz DG. A basic motif in the N-terminal region of RAG1 enhances V(D)J recombination activity. *Mol Cell Biol*. 1997;17:4544-4552.
- Roman CAJ, Cherry SR, Baltimore D. Complementmentation of V(D)J recombination deficiency in RAG-1<sup>-/-</sup> B cells reveals a requirement for novel elements in the N-terminus of RAG-1. *Immunity*. 1997;7:13-24.
- Kirch SA, Rathbun GA, Oettinger MA. Dual role of RAG2 in V(D)J recombination: catalysis and regulation of ordered Ig gene assembly. *EMBO J*. 1998;17:4881-4886.
- Noordzij JG, Verkaik NS, Hartwig NG, De Groot R, Van Gent DC, Van Dongen JJM. N-terminal truncated human RAG1 proteins can direct T-cell receptor but not immunoglobulin gene rearrangements. *Blood*. 2000;96:203-209.
- Roth DB, Roth SY. Unequal access: regulating V(D)J recombination through chromatin remodeling. *Cell*. 2000;103:699-702.
- Villa A, Santagata S, Bozzi F, et al. Partial V(D)J recombination activity leads to Omenn syndrome. *Cell*. 1998;93:885-896.
- Shinkai Y, Rathbun G, Lam KP, et al. RAG-2-deficient mice lack mature lymphocytes owing to inability to initiate V(D)J rearrangement. *Cell*. 1992;68:855-867.
- Mombaerts P, Iacomini J, Johnson RS, Herrup K, Tonegawa S, Papaioannou VE. RAG-1-deficient mice have no mature B and T lymphocytes. *Cell*. 1992;68:869-877.
- Gaspar HB, Conley ME. Early B cell defects. *Clin Exp Immunol*. 2000;119:383-389.
- Thompson A, Hendriks RW, Kraakman ME, et al. Severe combined immunodeficiency in man with an absence of immunoglobulin gene rearrangements but normal T cell receptor assembly. *Eur J Immunol*. 1990;20:2051-2056.
- Van Dongen JJM, Wolvers-Tettero ILM. Analysis of immunoglobulin and T cell receptor genes. Part I: basic and technical aspects. *Clin Chim Acta*. 1991;198:1-91.
- Noordzij JG, De Bruin-Versteeg S, Comans-Bitter WM, et al. Composition of the precursor B-cell compartment in bone marrow from patients with X-linked agammaglobulinemia compared to healthy children. *Pediatr Res*. 2002;51:159-168.

29. Verhagen OJHM, Wijkhuis AJM, Van der Sluijs-Gelling AJ, et al. Suitable DNA isolation method for the detection of minimal residual disease by PCR techniques. *Leukemia*. 1999;13:1298-1299.
30. Van Dongen JJM, Macintyre EA, Gabert JA, et al. Standardized RT-PCR analysis of fusion gene transcripts from chromosome aberrations in acute leukemia for detection of minimal residual disease. Report of the BIOMED-1 Concerted Action: investigation of minimal residual disease in acute leukemia. *Leukemia*. 1999;13:1901-1928.
31. Beishuizen A, De Bruijn MA, Pongers-Willems MJ, et al. Heterogeneity in junctional regions of immunoglobulin kappa deleting element rearrangements in B cell leukemias: a new molecular target for detection of minimal residual disease. *Leukemia*. 1997;11:2200-2207.
32. Szczepanski T, Pongers-Willems MJ, Langerak AW, et al. Ig heavy chain gene rearrangements in T-cell acute lymphoblastic leukemia exhibit predominant DH6-19 and DH7-27 gene usage, can result in complete V-D-J rearrangements, and are rare in T-cell receptor alpha beta lineage. *Blood*. 1999;93:4079-4085.
33. Pongers-Willems MJ, Seriu T, Stolz F, et al. Primers and protocols for standardized detection of minimal residual disease in acute lymphoblastic leukemia using immunoglobulin and T cell receptor gene rearrangements and TAL1 deletions as PCR targets. Report of the BIOMED-1 Concerted Action: investigation of minimal residual disease in acute leukemia. *Leukemia*. 1999;13:110-118.
34. Van der Burg M, Tumkaya T, Boerma M, De Bruin-Versteeg S, Langerak AW, Van Dongen JJM. Ordered recombination of immunoglobulin light chain genes occurs at the IGK locus but seems less strict at the IGL locus. *Blood*. 2001;97:1001-1008.
35. Lefranc MP, Giudicelli V, Ginestoux C, et al. IMGT, the international ImMunoGeneTics database. *Nucleic Acids Res*. 1999;27:209-212.
36. Pongers-Willems MJ, Verhagen OJ, Tibbe GJ, et al. Real-time quantitative PCR for the detection of minimal residual disease in acute lymphoblastic leukemia using junctional region specific Taq-Man probes. *Leukemia*. 1998;12:2006-2014.
37. Romanow WJ, Langerak AW, Goebel P, et al. E2A and EBF act in synergy with the V(D)J recombinase to generate a diverse immunoglobulin repertoire in nonlymphoid cells. *Mol Cell*. 2000;5:343-353.
38. Tsuganezawa K, Kiyokawa N, Matsuo Y, et al. Flow cytometric diagnosis of the cell lineage and developmental stage of acute lymphoblastic leukemia by novel monoclonal antibodies specific to human pre-B-cell receptor. *Blood*. 1998;92:4317-4324.
39. Groeneveld K, Te Marvelde JG, Van den Beemd MW, Hooijkaas H, Van Dongen JJM. Flow cytometric detection of intracellular antigens for immunophenotyping of normal and malignant leukocytes. *Leukemia*. 1996;10:1383-1389.
40. Van Lochem EG, Groeneveld K, Te Marvelde JG, Van den Beemd MW, Hooijkaas H, Van Dongen JJM. Flow cytometric detection of intracellular antigens for immunophenotyping of normal and malignant leukocytes: testing of a new fixation-permeabilization solution. *Leukemia*. 1997;11:2208-2210.
41. Wada T, Takei K, Kudo M, et al. Characterization of immune function and analysis of RAG gene mutations in Omenn syndrome and related disorders. *Clin Exp Immunol*. 2000;119:148-155.
42. Gomez CA, Ptaszek LM, Villa A, et al. Mutations in conserved regions of the predicted RAG2 kelch repeats block initiation of V(D)J recombination and result in primary immunodeficiencies. *Mol Cell Biol*. 2000;20:5653-5664.
43. Corneo B, Moshous D, Gungor T, et al. Identical mutations in RAG1 or RAG2 genes leading to defective V(D)J recombinase activity can cause either T-B-severe combined immune deficiency or Omenn syndrome. *Blood*. 2001;97:2772-2776.
44. Lucio P, Parreira A, Van den Beemd MW, et al. Flow cytometric analysis of normal B cell differentiation: a frame of reference for the detection of minimal residual disease in precursor-B-ALL. *Leukemia*. 1999;13:419-427.
45. Nomura K, Kanegane H, Karasuyama H, et al. Genetic defect in human X-linked agammaglobulinemia impedes a maturational evolution of pro-B cells into a later stage of pre-B cells in the B-cell differentiation pathway. *Blood*. 2000;96:610-617.